Thermal transport across incommensurate phases in potassium selenate: photo-pyroelectric and calorimetric measurements

2009 J. Phys.: Condens. Matter 21 045901

(http://iopscience.iop.org/0953-8984/21/4/045901)

J. Phys.: Condens. Matter **21** (2009) 045901 (6pp) doi:10.1088/0953-8984/21/4/045901

Thermal transport across incommensurate phases in potassium selenate: photo-pyroelectric and calorimetric measurements

J Philip and M V Manjusha

Sophisticated Test and Instrumentation Center, Cochin University of Science and Technology, Cochin 682 022, India

E-mail: jp@cusat.ac.in

Received 12 August 2008, in final form 31 October 2008
Published 15 December 2008
Online at stacks.iop.org/JPhysCM/21/045901

Abstract

The thermal transport properties—thermal diffusivity, thermal conductivity and specific heat capacity—of potassium selenate crystal have been measured through the successive phase transitions, following the photo-pyroelectric thermal wave technique. The variation of thermal conductivity with temperature through the incommensurate (IC) phase of this crystal is measured. The enhancement in thermal conductivity in the IC phase is explained in terms of heat conduction by phase modes, and the maxima in thermal conductivity during transitions is due to enhancement in the phonon mean free path and the corresponding reduction in phonon scattering. The anisotropy in thermal conductivity and its variation with temperature are reported. The variation of the specific heat with temperature through the high temperature structural transition at 745 K is measured, following the differential scanning calorimetric method. By combining the results of photo-pyroelectric thermal wave methods and differential scanning calorimetry, the variation of the specific heat capacity with temperature through all the four phases of K_2SeO_4 is reported. The results are discussed in terms of phonon mode softening during transitions and phonon scattering by phase modes in the IC phase.

1. Introduction

Since the discovery of ferroelectricity and successive phase transitions in potassium selenate (K_2SeO_4) single crystals, many experimental and theoretical studies have been carried out by different workers in efforts to understand the mechanisms of these transitions [1]. With the occurrence of the ferroelectric phase, this material also undergoes an incommensurate phase (IC phase) transition, which is of great interest to condensed matter physicists. Ferroelectric crystals which are known to exhibit IC phase transitions include ammonium fluoroberylate [2], potassium selenate [3], sodium nitrite [4], thiourea [5] etc. Potassium selenate, with the chemical formula K_2SeO_4, undergoes three successive phase transitions at temperatures $T_1 = 745$ K, $T_2 = 129.5$ K and $T_3 = 93$ K [1].

The crystal exhibits hexagonal structure in phase I, with space group D^4_{6h} $(P6_3/mmc)$ [6], which changes to an orthorhombic structure (phase II) with space group D^{16}_{2h} $(Pnam)$ at T_1 [7]. Then, phase II changes into an incommensurate one (phase III) at T_2 [3]; this is a second-order phase transition. It undergoes an IC phase transition at T_3, below which the crystal is commensurate and ferroelectric with a small spontaneous polarization along the c direction.

The existence of an IC phase and the transition to the commensurate phase has attracted the attention of many researchers to this crystal as a typical example exhibiting successive phase transitions with a clear IC phase. Many experimental studies such as dielectric measurements [1, 8], x-ray and neutron diffraction [3, 9, 10], ESR [11], Raman and Brillouin scattering [12–14], ultrasound velocity, attenuation and dispersion studies [15, 16] etc have been reported for near T_2 and T_3. The variations in specific heat capacity and thermal expansion of K_2SeO_4 in the low temperature phase have been reported by earlier workers [8, 20]. Thermal expansion along the c axis exhibits a discontinuity at the incommensurate to

commensurate transition. Specific heat measurements show anomalies at T_2 and T_3, indicating that the transition at T_2 is second order and that the one at T_3 is first order [8]. In spite of all these measurements reported at temperatures T_3 and T_2, only very few experimental results have been reported for near T_1 [17–20] because of the inherent difficulties involved in carrying out precision experiments at high temperatures. The variation of the specific heat capacity across the structural transition at T_1 has not been reported so far for this material. More experimental data are in fact still required for a better understanding of the high temperature phase of this material.

A dynamic measurement of the thermal conductivity across a transition temperature is rather difficult due to the fact that the sample cannot be kept in a steady state during measurements. Thermal wave measurements based on a photo-thermal effect, such as thermal wave interferometry, the photo-thermal deflection technique, photo-acoustic methods and photo-pyroelectric measurements help us to get over this difficulty. In these techniques one measures the thermal diffusivity, rather than thermal conductivity. Thermal diffusivity measurements do not suffer from heat losses from the sample during measurements and hence are more accurate than a direct measurement of thermal conductivity by the steady state method. With a proper choice of boundary conditions, photo-thermal/photo-acoustic techniques makes a simultaneous measurement of thermal diffusivity and effusivity possible, from which the thermal conductivity and specific heat capacity can be extracted. The photo-pyroelectric technique has been used earlier to measure the variations of thermal conductivity and heat capacity of a few crystalline solids as they undergo phase transitions with temperature [21, 22].

In this work we have measured the thermal diffusivity, thermal conductivity and heat capacity of K_2SeO_4 as it goes through the IC phase between 129.5 and 93 K. The anisotropy in thermal conductivity along the three principal directions of this crystal and its variation with temperature are brought out and discussed. Differential scanning calorimetric (DSC) measurements across the high temperature phases have been carried out to determine anomalies in enthalpy during the transition from phase I to phase II, and the calorimetric ratio method adopted to determine the variation of specific heat capacity with temperature across the high temperature transition point T_1. We have combined the results from photo-pyroelectric and calorimetric measurements to plot the variation of specific heat with temperature through all the four phases of K_2SeO_4, and the results are discussed.

2. Experimental method

2.1. Sample preparation

K_2SeO_4 crystals are grown from solution following the well known slow evaporation technique. Selenous acid (H_2SeO_3) is refluxed to get selenic acid (H_2SeO_4) using hydrogen peroxide. Then potassium carbonate and selenic acid are taken in stoichiometric proportions to get a solution of potassium selenate following the chemical reaction

$$K_2CO_3 + H_2SeO_4 \rightarrow K_2SeO_4 + CO_2 + H_2O.$$

The solution is kept in a bath for three to four weeks to get good transparent crystals of K_2SeO_4 of about $1 \times 1 \times 1$ cm^3 size. This crystal is isomorphous with $(NH_4)_2SO_4$ in morphology [20]. The x-ray powder diffraction pattern of the crystal, recorded for structure confirmation, agrees well with the earlier reported ones [3]. The crystals are cut with a slow speed diamond wheel saw in such a way that they have faces normal to the [100], [010] and [001] orientations of the crystal, which are designated as a, b and c axes respectively. The samples are carefully polished and made to have thickness of about 0.5 mm for photo-pyroelectric measurements. The density of the sample is measured to be 0.859 g cm^{-3}. Pieces of the crystal, weighing about 5 mg, are used for scanning calorimetric measurements.

The DSC and TG curves of the sample have been recorded over the entire temperature range of interest and compared with the corresponding curves reported in the literature. No extra peaks in the DSC curve or any other intermediate state in TG curve could be detected for the sample. If any impurity phase at all is present, it can be due to the presence of sulfur. We did plasma emission spectroscopic measurements on the sample to look for the presence of sulfur in the sample, but the result was negative. These results guarantee the phase purity of the sample(s) used for the measurements.

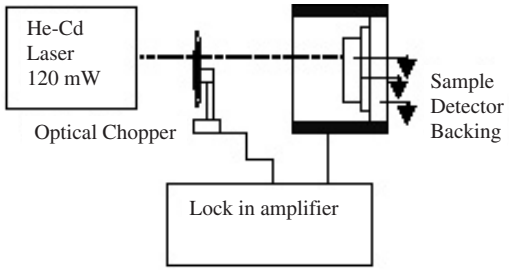

Figure 1. Block diagram of the experimental set-up used for PPE measurements.

2.2. Photo-pyroelectric thermal wave measurements

An improved photo-pyroelectric (PPE) technique has been used to determine the thermal properties of single crystals of K_2SeO_4 [21, 22]. For this measurement the sample thickness should be such that the sample, the pyroelectric detector and the backing material used are thermally thick during the measurement. The sample is illuminated with an intensity-modulated beam of light, which gives rise to periodic temperature variations in the sample via optical absorption. The thermal waves so generated propagate through the sample, and are detected with a pyroelectric detector. A block diagram of the experimental set-up used in the present experiments is shown in figure 1.

A 120 mW He–Cd laser of wavelength $\lambda = 442$ nm has been used as the optical heating source, and the intensity modulation is accomplished with a mechanical chopper

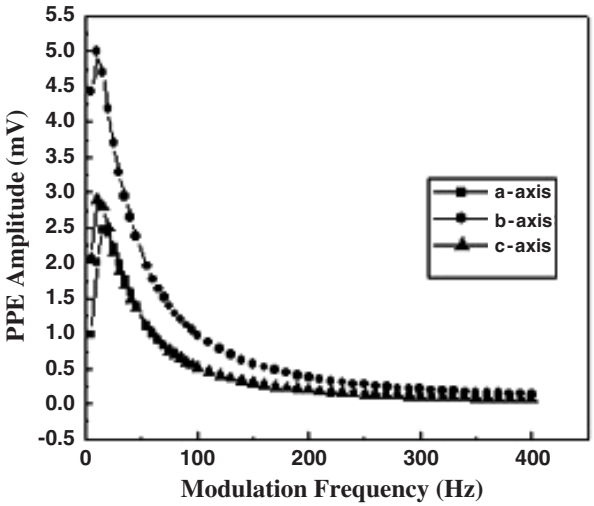

Figure 2. Frequency dependence of the photo-pyroelectric amplitudes along the three principal axes of K_2SeO_4 at room temperature.

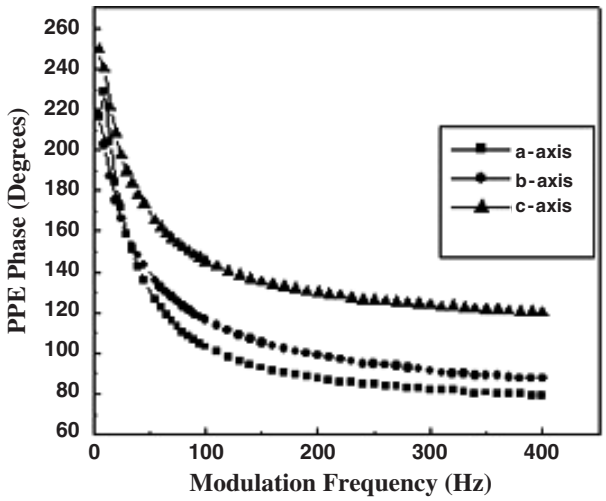

Figure 3. Frequency dependence of the photo-pyroelectric phases along the three principal axes of K_2SeO_4 at room temperature.

(Stanford Research Systems Model SR 540). A PVDF film of thickness 28 μm, with Ni–Cr coating on both sides, with a pyroelectric coefficient $P = 0.30 \times 10^{-8}$ V cm^{-1} K^{-1}, is used as the pyroelectric detector. The output signal is measured with a dual-phase lock-in amplifier (Stanford Research Systems Model SR 830). Modulation frequency is kept above 30 Hz in all our experiments to ensure that the detector, the sample and the backing medium are all thermally thick during measurements. The thermal thickness of the potassium selenate sample has been verified by plotting the variation in PPE amplitude and phase with modulation frequency at room temperature. Since the optical absorption in potassium selenate is low, a very thin coating of carbon black is carefully provided on the face of the sample under illumination to enhance optical absorption and consequent thermal wave generation.

Measurement of the PPE signal phase and amplitude enables one to determine the thermal diffusivity (α) and thermal effusivity (e) respectively. The principle of this method and experimental procedures are described in detail elsewhere [21]. From the measured values of α and e, the thermal conductivity k and specific heat capacity c_p of the sample are determined, knowing the density (ρ), using the following relations [21]:

$$k = e(\alpha)^{1/2} \tag{1}$$

$$c_p = e/(\rho(\alpha)^{1/2}). \tag{2}$$

The calibration of the experimental set-up has been done with known samples prior to carrying out measurements on K_2SeO_4. In photo-pyroelectric measurements, one measures the amplitude and phase of the pyroelectric detector output with the lock-in amplifier. These parameters are measured as a function of the modulation frequency to extract the thermal diffusivity and effusivity values of the sample. The sample temperature was kept constant during measurements, allowing sufficient time for the sample to reach thermal equilibrium.

These measurements have been done at temperatures between 85 and 300 K at temperature intervals of 2 K normally, and at intervals of 1 K at temperatures in the vicinity of the two transition points. First, measurements were done with the sample cut with faces normal to the c axis. At each measurement temperature, the sample was kept at a constant temperature during the measurement. From the frequency dependence of the pyroelectric amplitudes and phases, the thermal diffusivity and effusivity of the sample were determined at each temperature. These measurements were repeated for samples cut with faces normal to a as well as b axes.

2.3. Differential scanning calorimetric measurements

The DSC curve of the sample was plotted from 85 to 775 K with a Mettler Toledo DSC 822^e at a heating rate of 10 °C min^{-1}. In view of the fact that the low temperature transitions in K_2SeO_4 are weak, the variations in specific heat are comparatively small. It is difficult to measure such small variations with enough sensitivity following the DSC technique. In the high temperature region, the variation of specific heat with temperature has been determined by the ratio method with alumina used as the reference sample. This method results in specific heat capacity values with accuracies better than ±2.5%.

3. Results and discussion

The variations in PPE signal amplitude and phase measured as a function of modulation frequency for a K_2SeO_4 sample, measured along the three principal directions at room temperature, are shown in figures 2 and 3 respectively. Values of the thermal diffusivity and effusivity along the c axis, obtained from the PPE amplitude and phase values at each temperature, are plotted in figure 4. From the diffusivity and effusivity values, the corresponding values of the thermal conductivity and specific heat capacity have been computed,

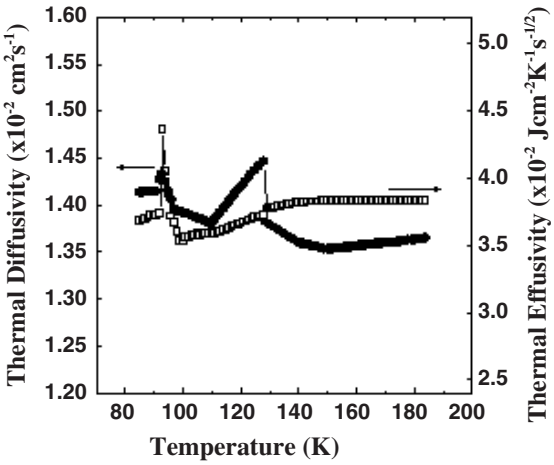

Figure 4. Variation of the thermal diffusivity and thermal effusivity along the c axis of K_2SeO_4.

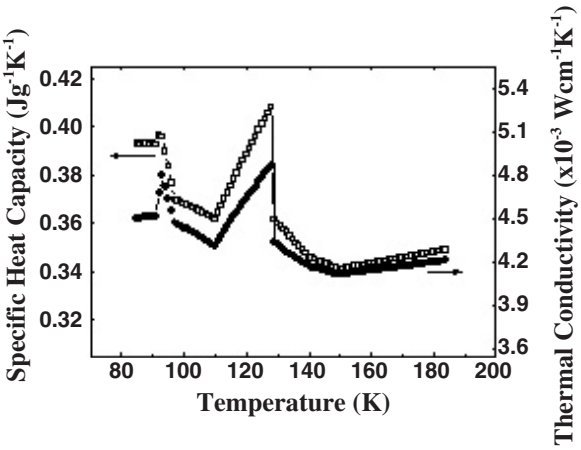

Figure 5. Variation of the thermal conductivity along the c axis and specific heat capacity of K_2SeO_4.

Table 1. Thermal conductivity (in units of W cm^{-1} K^{-1}) along the three principal axes of K_2SeO_4 at different temperatures.

	Thermal conductivity		
Temperature (K)	a axis	b axis	c axis
302 (Room temperature)	4.21 ± 0.01	4.22 ± 0.01	4.41 ± 0.01
127	4.86 ± 0.01	4.88 ± 0.01	5.10 ± 0.01
93	4.79 ± 0.01	4.78 ± 0.01	4.80 ± 0.01

and these are plotted in figure 5. Since the values of the above thermal parameters for the a and b axes are not very different from the corresponding values obtained for the c axis, they are not reproduced here. The numerical values of the thermal conductivity of K_2SeO_4 along the three symmetry axes at room temperature, as well as at 93 and 129.5 K, are tabulated in table 1. From this table one can estimate the anisotropy in thermal conductivity for potassium selenate at room temperature as well as at the two transition temperatures below room temperature. One can see that the thermal conductivity along the c axis, which is the direction of spontaneous polarization for this crystal, is slightly more than that along a or b axis at all temperatures. The anisotropy in thermal conductivity, in general, is small and decreases as the temperature is lowered. The thermal conductivity ellipsoids for all the three axes have been drawn with the corresponding thermal conductivity values at the two low temperature transitions as well as at room temperature to demonstrate the extent of the thermal conductivity anisotropy in this crystal. Since these ellipsoids are just circles without any anomalies, they are not reproduced here.

The variations in thermal diffusivity (α), effusivity (e), thermal conductivity (k) and specific heat capacity (c_p) with temperature along the c axis of K_2SeO_4, shown in figures 4 and 5, clearly indicate that the above thermal properties undergo anomalous variation during phase transitions at 93 and 129.5 K. Figure 5 clearly shows that the thermal conductivity and heat capacity exhibit maxima at the phase transition temperatures 93 and 129.5 K. Moreover, it can be seen that there is an overall enhancement in thermal conductivity in the IC phase of K_2SeO_4 between 93 and 129.5 K. The maxima in thermal conductivity at the phase transition temperatures can be explained in terms of the increase in phonon mean free path or decrease in phonon–phonon and phonon–defect collision rates. Again, the anomalous variation in specific heat capacity is due to softening of phonon modes and the corresponding enhanced contribution of phonon modes to the specific heat capacity.

The IC phase in K_2SeO_4 has been observed experimentally as satellite peaks in the x-ray and neutron diffraction patterns [3]. In the IC phase of K_2SeO_4 at temperatures close to T_2, the incommensurate modulation wave is pure harmonic. But as the temperature approaches T_3, nonlinear phase modes, which are equally spaced commensurate constant phase domains separated by narrow phase varying regions called phase solitons, emerge. The presence of these modulation waves or phase solitons can influence heat conduction in ferroelectric crystals in two different ways, as outlined below.

The general expression for thermal conductivity k in an insulating crystal is given by

$$k = (1/3)Cvl, \tag{3}$$

where C, v and l denote the phonon specific heat, the phonon group velocity and the phonon mean free path respectively. The phase solitons can affect the mean free path of thermal phonons via scattering and hence can cause anomalous variation of thermal conductivity in the IC phase. Another possibility is that the modulation waves themselves can act as heat carriers, resulting in an enhancement in thermal conductivity. Whether the thermal conductivity increases or decreases during an IC phase transition depends on which factor dominates in the process. One can isolate thermal conductivity enhancement in the IC phase by computing the value of $(k - k_{bg})$ where k is the total thermal conductivity and k_{bg} is the background thermal conductivity in the absence of the occurrence of IC modulation. In general, for an insulating crystal, k_{bg} follows an inverse T behavior.

The theory of heat conduction in a ferroelectric crystal with a two-component order parameter has been developed by Levanyuk and co-workers [23]. The theory considers heat conduction along the modulation axis of a system that undergoes IC phase transition. According to this, the thermal conductivity due to phase solitons is given by

$$k = k_{\mathrm{bg}} + (c_0^2 T \rho^2 / \gamma) \tag{4}$$

where c_0 and γ are constants, T is the temperature and ρ is the magnitude of the order parameter.

One can see that the phase solitons enhance the thermal conductivity K_2SeO_4 in the IC phase. It has also been shown that the enhancement in thermal conductivity is related to the excess specific heat c_{e} due to order parameter fluctuation as

$$\frac{\partial(k - k_{\mathrm{bg}})}{\partial T} \approx c_{\mathrm{e}}. \tag{5}$$

This explains the enhancement in specific heat in the modulation phase of the crystal. Even without the effects expressed in equations (4) and (5), the modulation waves can cause anomalies in $k - k_{\mathrm{bg}}$ by strongly scattering the heat carrying phonons.

In the IC phase between 93 and 129.5 K, one can note that the background thermal conductivity and the specific heat decrease gradually as the temperature increases. This variation of thermal conductivity is normal for a solid, but the variation of the specific heat is just opposite to the normal behavior for solids. This can be attributed to the increase in the heat capacity of the modulation waves with decrease in temperature. As the system approaches the low temperature commensurate phase, it becomes more and more ordered, resulting in a decrease in entropy or increase in heat capacity. The modulation waves are so strong in the IC phase that the contribution of modulation waves to the overall heat capacity of the system is much more than the contribution of normal phonon modes to heat capacity. This results in an overall increase in heat capacity as the temperature decreases in the IC phase.

The DSC curve during the heating cycle shows a clear peak occurring at 745 K, indicating that the phase transition at this temperature is endothermic. The variation of specific heat capacity with temperature up to a temperature well above 745 K has been determined by the DSC ratio method. These results have been combined with the results shown in figure 5 to plot the variation of heat capacity with temperature encompassing all the four phases of K_2SeO_4. This is shown in figure 6. To the best of our knowledge, this is the first time the variation of the specific heat of K_2SeO_4 through all the three transition temperatures T_1, T_2 and T_3 (and through all the four phases) has been plotted. The anomalous variation in heat capacity during transitions can be understood as due to softening of the phonon modes and the corresponding enhanced contribution of phonon modes to the specific heat capacity of the system.

In order to estimate the quantity of excess heat capacity due to the structural phase transition at 745 K, the contribution of the normal heat capacity must be subtracted from the measured molar heat capacity. The background lattice heat capacity was approximated by a third-order polynomial. The excess of the molar heat capacity ΔC_p was plotted against $T - T_{\mathrm{c}}$ and it is found to have a shape typical for a continuous phase transition. At $T = T_{\mathrm{c}}$, ΔC_p is found to be 0.112 ± 0.003 J K^{-1} mol^{-1}. The specific heat critical exponent α was obtained from the slope of $\log(\Delta C_p)$ versus $\log(T - T_{\mathrm{c}})$. The value of α is found to be -0.0853 ± 0.0002, which is close to zero. This value of the critical exponent α is typical for a mean field model of a phase transition [24]. The Landau theory gives a simple relation between the excess entropy and the order parameter P_{s} (spontaneous polarization): given by

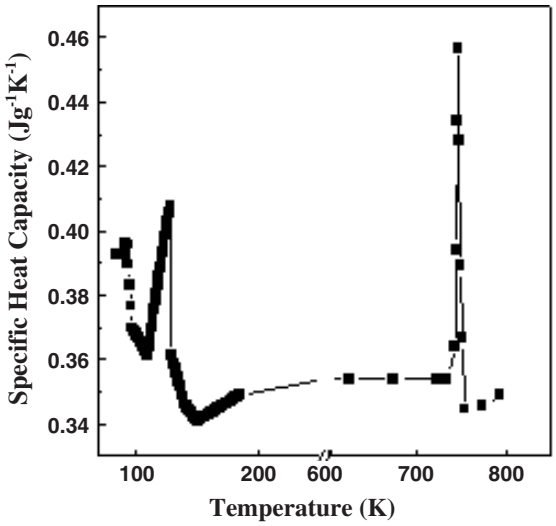

Figure 6. Variation of the specific heat capacity with temperature through all the four phases of K_2SeO_4. The inset shows the variation close to the high temperature transition point.

$$\Delta S(T) = -(1/2)[A_0 P_s^2]. \tag{6}$$

One can acquire more information about the nature of the phase transition from the excess entropy ΔS. The most direct way to determine ΔS is from the measurement of the excess beat capacity as a function of temperature:

$$\Delta S(T) = \int_{T_0}^{T} \frac{\Delta C_p}{T}\,\mathrm{d}T. \tag{7}$$

The transition entropy has been calculated from the above equation, and is obtained as $\Delta S = 0.49 \pm 0.03$ J K^{-1} mol^{-1}. This is typical of a structural phase transition. However, this is much smaller than the transition entropy predicted by the order–disorder model in the mean field theory. Other mechanisms such as tunneling may have to be taken into account to reduce this discrepancy with experiment.

Acknowledgments

The authors thank the Sophisticated Analytical Instrument Facility, Cochin, for help with TG/DSC and XRD measurements. One of the authors (MVM) thanks Cochin University of Science and Technology for a fellowship.

References

[1] Aiki K, Hukuda K and Matumura O 1969 *J. Phys. Soc. Japan* **26** 1064
[2] Iizumi M and Gesi K 1977 *Solid State Commun.* **22** 37
[3] Iizumi M, Axe J D, Shirane G and Shimaoka K 1977 *Phys. Rev.* B **15** 4392
[4] Yamada Y, Shibuya I and Hoshino S 1963 *J. Phys. Soc. Japan* **18** 1594
[5] Goldsmith G J and White J G 1959 *J. Chem. Phys.* **31** 1175
[6] Shiozaki S, Sawada A, Ishibashi Y and Takagi Y 1977 *J. Phys. Soc. Japan* **43** 1314
[7] Kálmán A, Stephens J S and Cruickshank D W J 1970 *Acta Crystallogr.* B **26** 1451
[8] Aiki K, Hukuda K, Koga H and Kobayashi T 1970 *J. Phys. Soc. Japan* **28** 389
[9] Ohama N 1974 *Mater. Res. Bull.* **9** 283
[10] Terauchi H, Takenaka H and Shimaoka K 1975 *J. Phys. Soc. Japan* **39** 435
[11] Aiki H 1970 *J. Phys. Soc. Japan* **29** 379
[12] Wada M, Sawada A, Ishibashi Y and Takagi Y 1977 *J. Phys. Soc. Japan* **42** 1229
[13] Wada M, Uwe H, Sawada A, Ishibashi Y, Takagi Y and Sakudo T 1977 *J. Phys. Soc. Japan* **43** 544
[14] Yagi T, Cho M and Hidaka Y 1979 *J. Phys. Soc. Japan* **46** 1957
[15] Hoshizaki H, Sawada A, Ishibashi Y, Matsuda T and Hatta I 1980 *Japan. J. Appl. Phys.* **19** L324
[16] Shiozaki S, Sawada A, Ishibashi Y and Takagi Y 1977 *J. Phys. Soc. Japan* **43** 1314
[17] Unruh H G, Eller W and Kirf G 1979 *Phys. Status Solidi* a **55** 173
[18] Inoue K, Suzuki K, Sawada A, Ishibashi Y and Takagi Y 1979 *J. Phys. Soc. Japan* **46** 608
[19] Cho M and Yagi T 1980 *J. Phys. Soc. Japan* **49** 429
[20] Gupta S S, Karan S and Gupta S P S 2000 *Japan. J. Appl. Phys.* **39** 2736
[21] Menon C P and Philip J 2000 *Meas. Sci. Technol.* **11** 1744
[22] Marinelli M, Murtas F P, Mecozzi M G, Zammit U, Pizzoferrato R, Scudierri F, Maerwllucci S and Marinelli M 1990 *Appl. Phys.* A **51** 387
[23] Levanyuk A P, Minyukov S A and Vallade M 1992 *J. Physique* I **2** 1949
[24] Strukov B A and Levanyuk A P 1998 *Ferroelectric Phenomena in Crystals* (Berlin: Springer)